Evaluation of the Reliability of a Novel ICPC Solar Collector Installation: Incorporating the Diffuse Radiation Component into the Analysis and Its Impact on the Comparison between Measured and Predicted Performance

William S. Duff* and Jirachote Daosukho
Department of Mechanical Engineering, Colorado State University, Ft. Collins CO 80523
* Corresponding Author, bill@engr.colostate.edu

Abstract

A novel integral compound parabolic concentrator evacuated solar collector (ICPC) array has been in continuous operation at a demonstration project in Sacramento California since 1998. An ongoing study addresses the impact of optical, thermal, degradation and component failure factors on array performance over the eleven years of operation. This paper reports on how two primary failure modes have affected optical and thermal performance of the evacuated tubes and the array.

In 1998 and 1999, while operating in the range of 120 to 160C, daily collection efficiencies of nearly 50 percent and instantaneous collection efficiencies of about 60 percent were achieved. Daily chiller COPs of about 1.1 were achieved and the two differently oriented collector absorber fins gave essentially identical performance.

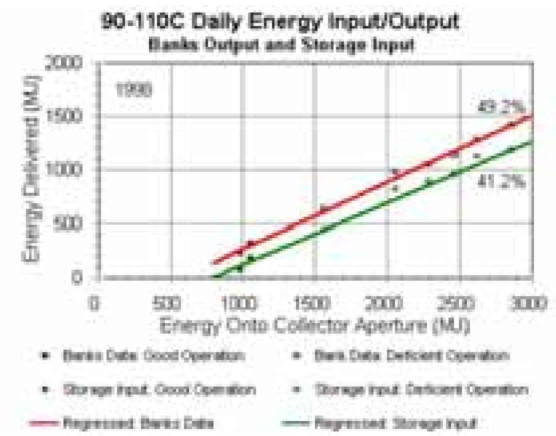

Fig. 1. 1998 daily collection performance for operation at 90 to 110C collector to ambient temperature differences.

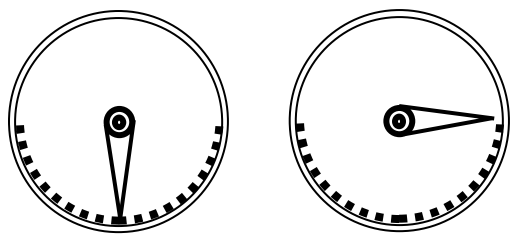

Fig. 2. Novel ICPC design showing vertical and horizontal fin orientations.

A 3-dimention animated graphical ray tracing simulation tool was developed to investigate changes to the incidence angle modifier of the ICPC for the vertical and horizontal absorber fin orientations. Since ICPCs collect a fair amount of energy during cloudy day or mostly diffuse radiation, a separated simulation program is designed to capture diffuse elements of the radiation which is assumed to be coming from all direction from the hemisphere to the collector. Beam and diffuse radiation contribution to overall radiation is also estimated to match the actual experimental climate. The device consists of a laser and detector mounted on a support structure that can be positioned on the various tubes of the ICPC array to measure transmittance and reflectance losses. Using this device, a map of reflector performance for the ICPC array has been generated.

The paper will include a review of collection system performance and reliability over the twelve years of operation, animations of rays striking at various angles, the incidence angle evaluation. Results in this paper are 1) the modeling and analysis for off-normal incident rays for both the vertical and horizontal fin orientations, 2) Beam/Diffuse radiation contribution to overall radiation, 3) diffuse efficiency between the two ICPC fin alignments, 4) the reflectance measurement results and the reflectance degradation map, 5) a comparison with the experimental results for both the vertical and horizontal absorber fins and 6) an analysis of the of the effects of the two fin orientations and two failure modes on performance.

Keywords: ICPC, Optical Modeling, Materials Degradation, Reliability

1. Background

1.1. Development of the novel ICPC

Research on CPC solar collectors has been going on for almost thirty years. See Garrison [1] and Snail et al [2]. In the early 1990s a new ICPC evacuated collector design was developed. The new ICPC design allows a relatively simple manufacturing approach and solves many of the operational problems of previous ICPC designs. The design, fabrication and testing approaches are described in Duff et al [3] and Winston et al [4].

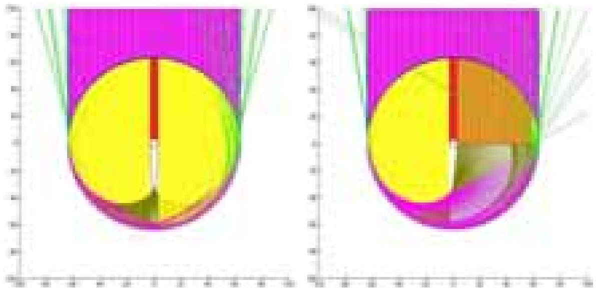

Fig.3. Projected rays at normal incidence on both vertical and horizontal fins configuration

1.2. Sacramento demonstration

A 100 m2 336 Novel ICPC evacuated tube solar collector array has been in continuous operation at a demonstration project in Sacramento California since 1998. The evacuated collector tubes are based on a novel ICPC design that was developed by researchers at the University of Chicago and Colorado State University in 1993. The evacuated collector tubes were hand-fabricated from NEG Sun Tube components by a Chicago area manufacturer of glass vacuum products.

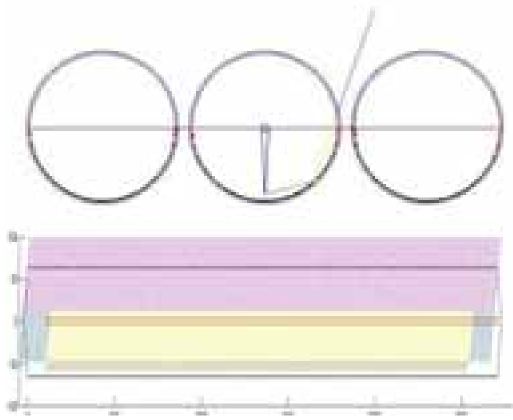

Fig.4. Projected rays on both transverse and longitudinal views on vertical fin ICPC

From 1998 through 2002 demonstration project ICPC solar collectors supplied heated pressurized 150C water to a double effect (2E) absorption chiller. The ICPC collector design operates as efficiently at 2E chiller temperatures (150C) as do more conventional collectors at much lower temperatures. This new collector made it possible to produce cooling with a 2E chiller using a collector field that is about half the size of that required for a single effect (1E) absorption chiller with the same cooling output. Data collection and analysis has continued to the present [5, 6, 7, 8].

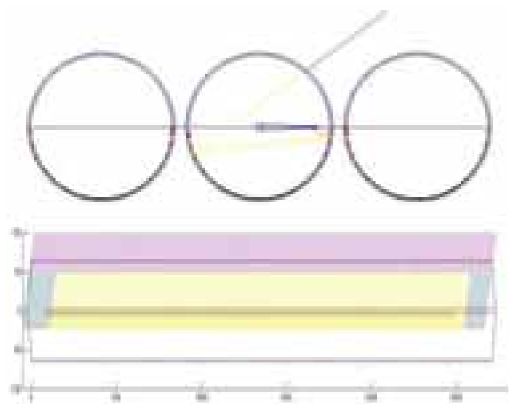

Fig.5. Projected rays for both transverse and longitudinal views for the horizontal fin ICPC

As can be seen in Fig. 1, the non-tracking ICPC evacuated solar collector array provided daily solar collection efficiencies (based on the total solar energy falling on the collector) approaching fifty percent and instantaneous collection efficiencies of about 60 percent at the 140C to 160C collector operating temperature range. Daily chiller COPs of about 1.1 were achieved. The ICPC array has recently been operating at the lower temperatures to drive a single effect absorption chiller. The ICPC array has provided daily solar collection efficiencies approaching fifty-five percent at the 80C to 100C collector operating temperature range.

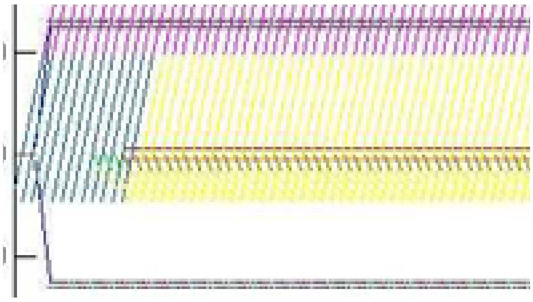

Fig.6. Close-up of projected rays in the longitudinal view with multiple reflections

Table 1. Color codes to illustrate ray action

Color	Code
Pink	Ray enters outer glass tube
Red	Ray hits heat transport tube
Blue	Ray missing aperture area
Yellow	Ray hits reflective surface
Brown	Ray hits absorber fin
Green	Ray is reflected out

1.3. Array layout and absorber orientation

The new ICPC evacuated tubes were fabricated with two absorber orientations, one with a vertical absorber fin and one with a horizontal fin. A cross-section of the collector tube illustrating the two orientations is shown in Fig. 2.

Fig.7. Fourth level reflectance degradation.

The vertical fin configuration has a symmetric configuration, which has the advantage of being symmetrical, but the disadvantage that almost all of the light must be reflected onto the absorber since the most of the surface area of the absorber fin is located in the shadow of the absorber tube above, Figure 3. An alternative asymmetric horizontal fin configuration has the same effective geometric concentration and the same thermal loss characteristics but higher expected optical efficiency with a lower average number of reflections at normal incidence as shown in Figure 3. At normal incidence sunlight, more than half the aperture area of the sun radiation falls directly on the top absorber surface without reflection. ICPC tubes with this horizontal orientation fin maintain the optical, thermal, and manufacturability advantages of the vertical fin orientation. However, it is believed that the lower average number of reflections might lead to better overall performance, so approximately half of the tubes were produced in each orientation, and modules of each configuration were tested at Sandia, Winston et al. [4].

The collector array is made up of three banks. The north bank consists of all horizontal fin tubes, the middle bank consists of all vertical fin evacuated tubes and the south bank includes an even mixture of the two types. The two differently oriented fined collectors gave essentially identical performance. The flow pattern through the 112 evacuated tubes in each bank is parallel and the three banks are plumbed in parallel.

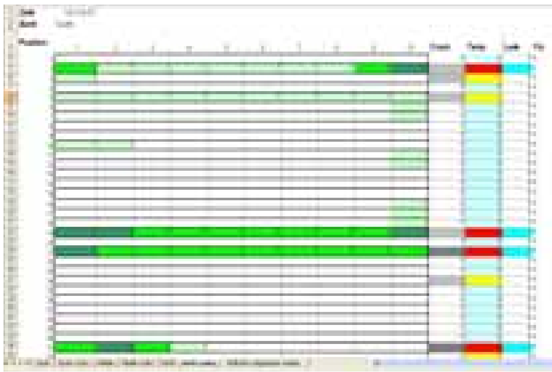

Fig.8. Map of tube degradation

2. Optical Performance Modeling and Experimentation

2.1. Graphical ray tracing

Fig. 4 depicts the results of an animated graphical ray tracing simulation that has been designed to investigate the optical performance of the ICPC. See Duff, et al [7]. Factors incorporated are the transmittance of the glass tube, the reflectivity of the reflective surface, the gap between the tube surface and the fin and the absorptance of the fin. The sun rays are simulated as discrete uniform rays over a range of incident angles from 15 degrees to 165 degrees. The rays are followed through the glass envelope, to the reflector and to the absorber fin. The number of rays absorbed is recorded.

Table 2. Measurement of reflectivity

Degradation Level	Percent Reflectivity
Good	93.48
1st	79.66
2nd	38.46
3rd	22.93
4th	1.24

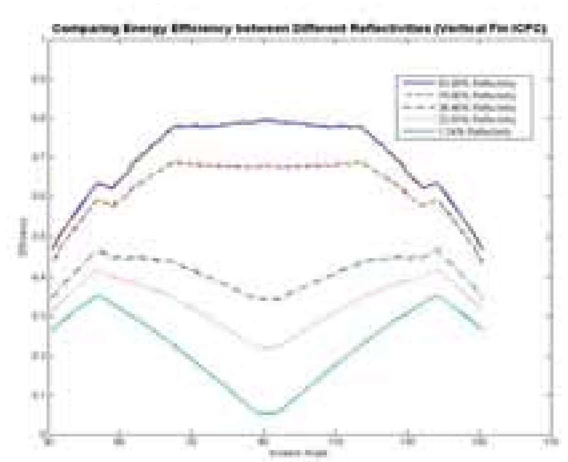

Fig.9. Comparing optical efficiency between different reflectivity ratios (vertical fin)

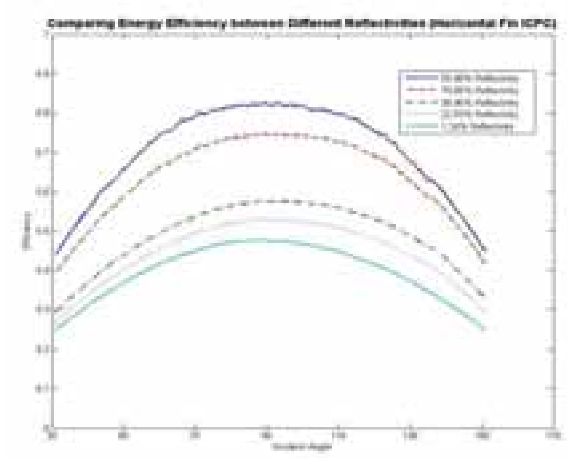

Fig.10. Comparing optical efficiency between different reflectivity ratios (horizontal fin)

2.1.1. Three dimensional ray tracing

The projected solar radiation is analyzed in the terms of both longitudinal and transverse incident angles to the tube. The reference axis is adjusted to be in the same plane as the collector plane.

As shown in the longitudinal view, the simulation follows each ray in the transverse view as a uniformly distributed set of rays. A ray striking the collector at a given angle and in given location is monitored as to how it responds at various surfaces and orientations of the collector. A color code shown in Table 1 provides a means of following how simulated rays respond at the various surfaces.

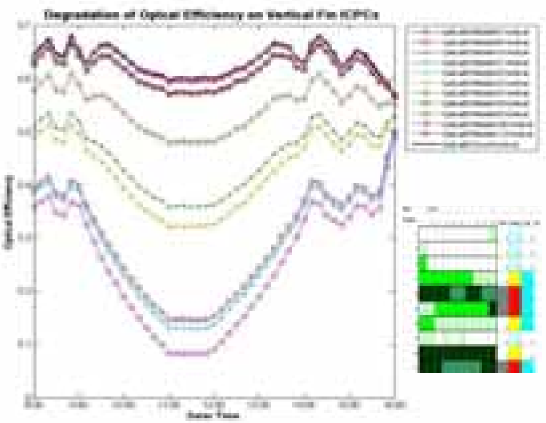

Fig.11. Matching optical efficiency with degradation map from middle bank (vertical fin)

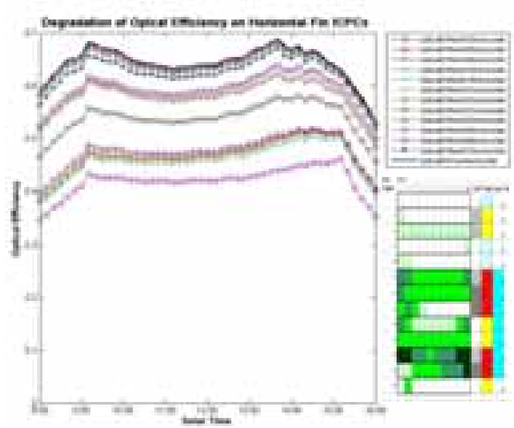

Fig.12. Matching optical efficiency with degradation map from north bank (horizontal fin)

Figure 3 shows an individual ray traced in the transverse plane projected to the longitudinal plane as an array of uniformly distributed rays. The ray tracing procedure is set up to trace individual rays and their intensities until one hits the absorber plate or is reflected out. The direction of the ray travelling in the ICPC tube is recorded and projected into both transverse and longitudinal views.

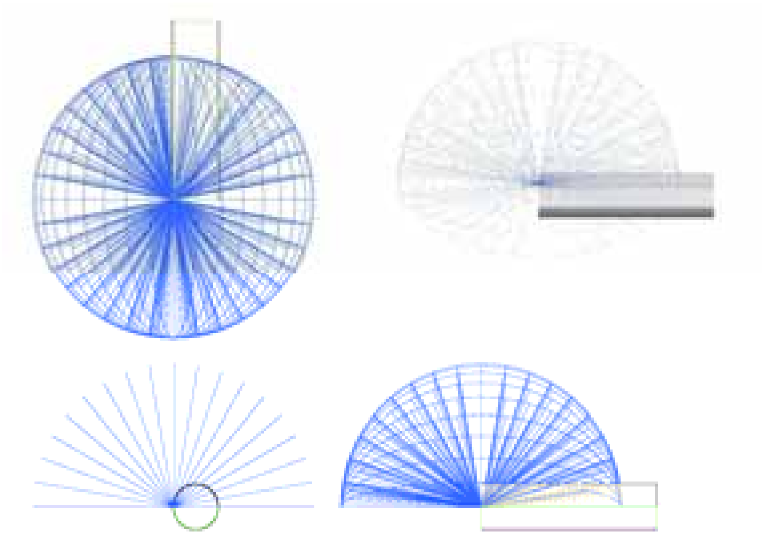

Fig.13. Projected diffuse ray elements on multiple views

When each ray is traced on the transverse plane, the uniform distribution of rays is analyzed throughout the longitudinal view. Each ray is followed starting from where it enters the tube in the transverse plane. The pink color code will mark the ray from outside glass cover to the entrance point. After the rays (pink colored) enter the tube longitudinally, each ray will be followed to see if it hits or misses the reflector. The rays that miss the reflector or absorber are then colored blue. The remaining rays then hit the reflector, perhaps multiple times, before hitting the absorber or being reflected out of the glass tube.

The reflected angle in the longitudinal view is calculated by using its recorded last reflected position from the transverse view and this is then applied to the longitudinal view. At this point each reflected ray is color coded yellow. After this reflection, each ray is followed and investigated to see if it hits the absorber (brown) or reflected out (green). See Fig. 5 and 6.

2.2. Reflectivity measurement

A device, consisting of a laser and detector mounted on a support structure is used to measure reflectance of mirror surface samples from the ICPC. Using this device, a map of reflector performance that is keyed to the appearance of the reflective surface for the tubes in ICPC array has been generated. Four levels of reflectance degradation are identified for the Sacramento site by the appearance of the reflective surface. At level 1 the reflector still performs well and only a minor change in the reflector appearance is observed. At level 2 there is some whitening of the reflector. At level 3 there is a substantial amount of degradation of the reflector. At level 4, shown in Fig. 7, most of reflector is gone and you can easily see through it.

At the site, all 336 tubes were categorized, one-by-one, by the above reflectivity appearance levels, existence of a glass crack, surface temperature, water leakage, and fin orientation. Each tube was divided into ten sections along its length. Degradation levels were identified and marked for each of the ten sections. Fig. 8 shows a color mapping of tube degradation information for a portion of the array.

Reflector samples representative of the four different degradation levels were taken from the Sacramento site to the laser laboratory at Colorado State University. The samples for the four levels of degradation and good reflector samples were measured for their reflectivity by the laser detection device. Using this device, a map of reflector performance for the ICPC array is being generated. The reflectance results are shown in Table 2 for each level of degradation.

2.3 Effects of two fin orientations and two failure modes on performance

Reflectivity degradation plays an important role on the performance of the evacuated tube. As reflectivity degrades, the performance of tubes with the two fin orientations falls off in different ways. For the vertical fin, performance drops rapidly for incidence angles close to 90 degrees. This behavior is as expected since the vertical fin receives

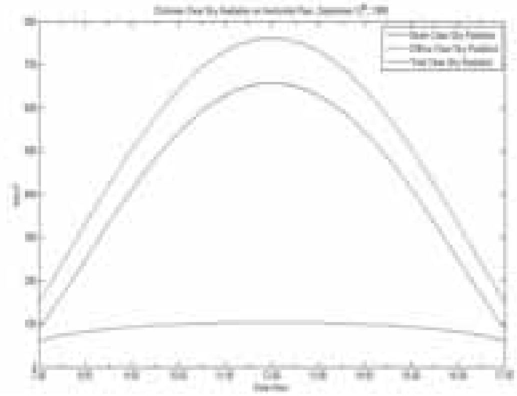

Fig.14. Estimated clear sky radiation (beam and motion) on the horizontal for Sept. 12th 1999

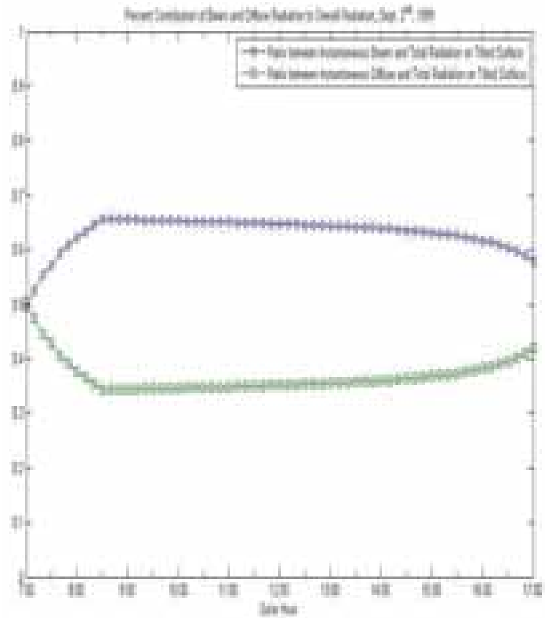

Fig.15. Percent contribution of beam and diffuse radiation to overall radiation on September 2nd 1999

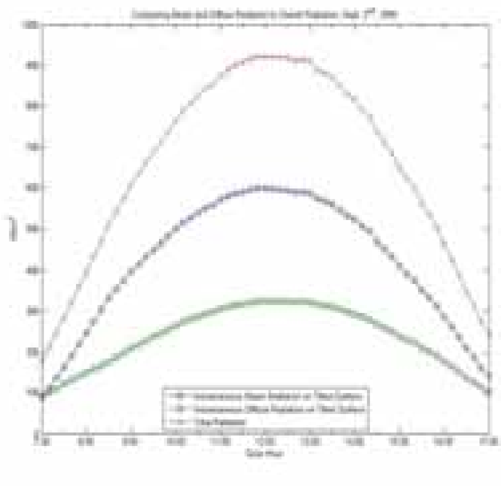

Fig.16. Beam and diffuse radiation to overall radiation September 2nd 1999

radiation mostly from the reflector. The horizontal absorber fin performs better than vertical absorber fin when the reflector degrades since the horizontal fin absorbs some of the radiation directly, Fig. 9 and Fig 10.

Next, the degradation map from the actual site in Sacramento is included into the three dimensional ray tracing simulation. The simulation allows us to customize different reflectivity into each section on the longitudinal view. Figure 11 and 12 show how the optical efficiency is turning out as the investigated reflector degradation characteristic of each ICPC tube is matched.

2.4 Diffuse ray-tracing simulation

Assuming that diffuse rays will come from all available direction of the hemisphere perpendicular to the collector, the diffuse ray-tracing simulation is designed to capture rays cast from uniformly distributed points on the hemisphere to each point on the collector. These points on the collector are uniformly distributed throughout its effective area. See Fig.13. As each ray is traced, it loses intensity from transmittance and reflectance losses before hitting an absorber fin or being reflected out. This is the same process as was described in the beam ray-tracing simulation.

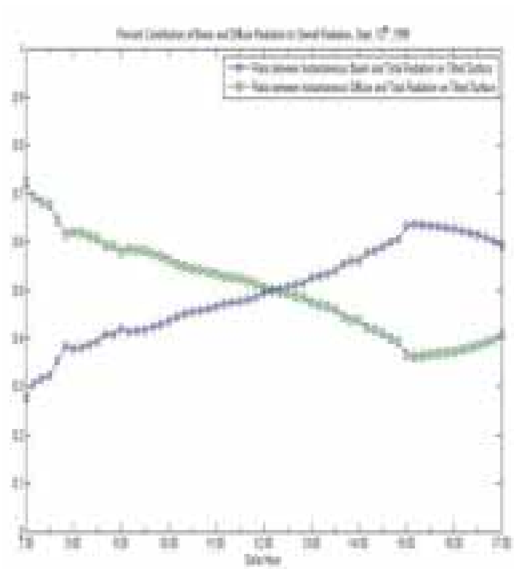

Fig.17. Percent contribution of beam and diffuse radiation to overall radiation, September 12th 1999

2.5 Beam/diffuse radiation contribution to overall radiation estimation

Finding the proportion of beam versus diffuse radiation in overall radiation is an important issue in the ray-tracing simulation analysis and is necessary to determine how each type of radiation influences optical efficiency. Total clear sky radiation is estimated by determining the atmospheric transmittance of beam and diffuse radiation. The atmospheric transmittance for beam radiation can be estimated by using a method presented by Hottel [9]. Fig. 14 illustrates beam and diffuse components of clear sky radiation. The estimated diffuse radiation is close to a constant with small dips at the beginning and the end of the day.

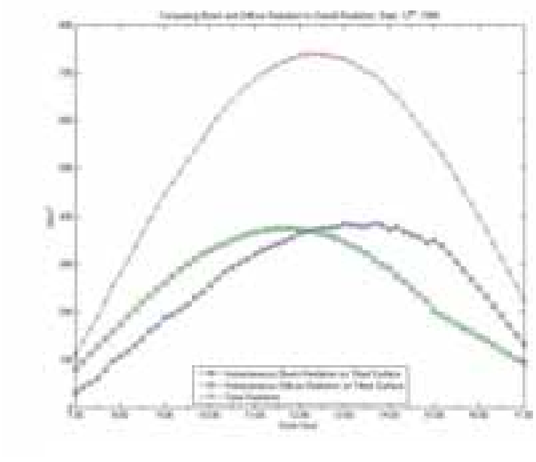

Fig.18. Beam and diffuse radiation to overall radiation September 12th 1999

By comparing measured and estimated clear sky radiation, the beam and diffuse components of clear and cloudy day radiation may be found. Stauter and Klien [10] developed a correlation between a proportion of diffuse radiation and measured radiation I_d/I (G_d/G_H) and a proportion of measured radiation and clear sky radiation I/I_c (G_H/G_c), on an hourly radiation (or instantaneous radiation) basis.

Beam and diffuse components of total radiation on a tilted surface are estimated by using the equation from Liu and Jordan [11]. They proposed that the radiation on tilted surface consists of three components: beam radiation, diffuse solar radiation, and solar radiation diffusely reflected from the ground with diffuse ground reflectance. Accordingly, total solar radiation on the tilted surface can be written as

$$I_T = [I_b R_b] + \left[I_d \left(\frac{1+\cos\beta}{2} \right) \right] + \left[(I_b + I_d)\rho \left(\frac{1-\cos\beta}{2} \right) \right]$$

where the proportion of beam radiation on the tilted surface, R_b, is

$$R_b = \frac{\cos(\phi-\beta)\cos\delta\cos\omega + \sin(\phi-\beta)\sin\delta}{\cos\phi\cos\delta\cos\omega + \sin\phi\sin\delta}$$

The ground albedo ρ is recommended to be taken as 0.2 when there is no snow cover and 0.7 when there is fresh snow.

The diffuse solar radiation and solar radiation diffusely reflected from the ground can be added together as I_{Td}. Rewriting the ratio between instantaneous beam radiation on a tilted surface, G_{Tb} and instantaneous total radiation on tilted surface, G_T we have

$$\frac{G_{Tb}}{G_T} = \frac{[G_b R_b]}{G_T}$$

and the ratio between instantaneous diffuse radiation on a tilted surface G_{Td} and instantaneous total radiation on a tilted surface, G_T,

$$\frac{G_{Td}}{G_T} = \frac{\left[G_d \left(\frac{1+\cos\beta}{2} \right) \right] + \left[(G_b + G_d)\rho \left(\frac{1-\cos\beta}{2} \right) \right]}{G_T}$$

The percentage contribution beam and diffuse elements to overall radiation for September 2nd 1999 are plotted to show these contribution characteristics during particular day. Fig. 15 and 16 show an equal contribution between beam and diffuse in the early morning. The sky then begins to clear during the rest of the day with a greater beam radiation contribution. For September 12th a greater percentage of diffuse radiation occurred in the earlier part of the day then the sky cleared up with the beam contribution becoming greater than the diffuse contribution later in the evening. See Fig. 17 and 18. This can be interpreted as a high diffuse or cloudy condition in the morning. Later in the day, the beam contribution became higher as the weather and visibility improved. The percent contributions of beam and diffuse radiation are then applied in the instantaneous optical efficiency analysis.

3. Conclusions

A detailed ray trace analysis for characterizing the optical performance of ICPC evacuated tubes and its extension to diffuse radiation has been described and the results illustrated. Through ray tracing analysis it was found that the nature of reflectivity degradation will play a significant role in the reduction of array efficiency. The nature of reflectivity degradation depends on the fin orientation and the type of failure, such as water leakage from the heat transport tube or cracks in the cover glass. Overall performance is also affected by loss of vacuum in the evacuated tube. An analysis of the performance consequences of reflector degradation and loss of vacuum is currently being incorporated into the reliability study and will be compared with collected performance data.

References

(1) Garrison, J. D., Optimization of Fixed Solar Thermal Collectors, *Solar Energy*, vol. 23, 1979

(2) Snail, J. J., O'Gallagher and R. Winston, A Stationary Evacuated Collector with Integrated Concentrator, *Solar Energy*, vol. 33, 1983.

(3) Duff, William S, R. Duquette, Roland Winston and Joseph O'Gallagher Development, Fabrication and Testing of a New Design for the Integrated Parabolic Evacuated Collector, Proceedings of the ASES/ASME Solar Energy Forum, Washington D. C. April, 1997.

(4) Winston, R, O'Gallagher, J., Mahoney, A. R., Dudley, V. E. and Hoffman, R., "Initial Performance Measurements from a Low Concentration Version of an Integrated Compound Parabolic Concentrator (ICPC)", Proceedings of the 1999 ASES Annual Conference, Albuquerque NM, June, 1998.

(5) Duff, William, Roland Winston, Joseph O'Gallagher, Tom Henkel and Jim Bergquam, "Performance of the Sacramento Demonstration ICPC Collector and Double Effect Chiller in 2000 and 2001", *Solar Energy*, vol. 76, pages 175-180, January 2004.

(6) Duff, William, Jirachote Daosukho, Klaus Vanoli, Roland Winston, Joseph O'Gallagher, Tom Henkel and Jim Bergquam, "Comparisons of the Performance of Three Different Types of Evacuated Tubular Solar Collectors", American Solar Energy Society 2006 Congress, Denver, Colorado, July 2006.

(7) Duff, William S. and Jirachote Daosukho, "Eleven Year Evaluation of a Novel ICPC Solar Collector Installation: The Role of Failure Modes in Changing Optical and Thermal Performance", American Solar Energy Society 2008 Congress, Buffalo NY, May 2009.

(8) Duff, William S, Jirachote Daosukho and Bengt Perers, "Three Dimensional Ray Tracing and Reliability Analyses of a Novel ICPC Collector after Twelve Years Of Operation", 2010 SWC Eurosun Congress, Graz, Switzerland, September 27-29, 2010.

(9) Hottel, H. C., "A Simple Model for Estimating the Transmittance of Direct Solar Radiation Through Clear Atmospheres", *Solar Energy*, 18, 129(2976).

(10) Stauter, R. and S. A. Klien, Personal communication (1979), mentioned in Duffie and Beckman, Solar Engineering of Thermal Processes.

(11) Lui, B. Y. H. ans R. C. Jordan, "The Long-Term Average Performance of Flat-Plate Solar Energy Collectors", *Solar Energy*, 7, 53(1963).